pected (that is, π out of phase). This difference becomes even more apparent when we compare the top insets in Fig. 3, A and B, which represent the calculated interferogram amplitudes in the absence of dephasing for the parameters obtained from fitting the data points (*26*).

The excited state coherence of the artificial "atom" studied here has a decoherence time of 40 ps, which is short compared with atomic coherence times, thus limiting the use of these particular QDs for quantum logic. However, very long electronic spin coherence in semiconductors has recently been measured (*27*). Furthermore, QD structures with stronger confinement are expected to have reduced coupling to phonons (*28*) and reduced spontaneous radiative emission (*29*), and may well have much longer intrinsic coherence times. In addition, doping of dots may result in isolated impurity states with long coherence times associated with more complex states of excitation such as demonstrated in atomic systems (*30*). Such progress should allow the use of more complicated sequences of control pulses during the coherence time, such as those necessary for performing quantum logic (*5*) or other coherently controlled processes.

The measurements show that we have successfully demonstrated coherent optical control of the quantum state of a single dot and thus have taken this technique to the ultimate quantum limit. We show that we can extend such an experiment to include more than one excited state and monitor the wave function as it oscillates between two orthogonal states by measuring the autocorrelation function. Finally, we show the feasibility of generating a target wave function by demonstrating control over the quantum mechanical phase of the superposition of states. This work establishes the basic tools for developing more sophisticated control and for creating a more complex wave function such as achieved in atomic systems.

Reference and Notes

1. A. P. Alivisatos, *Science* **271**, 933 (1996).
2. K. Brunner *et al., Phys. Rev. Lett.* **73**, 1138 (1994); H. F. Hess *et al., Science* **264**, 1740 (1994).
3. D. Gammon *et al., Science* **273**, 87 (1996).
4. G. Schedelbeck, W. Wegscheider, M. Bichler, G. Abstreiter, *ibid.* **278**, 1792 (1997); S. A. Empedocles and M. G. Bawendi, *ibid.*, p. 2114; D. Gammon *et al., ibid.* **277**, 85 (1997); J. Hasen *et al., Nature* **390**, 54 (1997); E. Dekel *et al., Phys. Rev. Lett.* **80**, 4991 (1998); L. Landin *et al., Science* **280**, 262 (1998).
5. S. Lloyd, *Science* **261**, 1569 (1993); A. Barenco, D. Deutsch, A. Ekert, R. Jozsa, *Phys. Rev. Lett.* **74**, 4083 (1995); A. Ekert and R. Jozsa, *Rev. Mod. Phys.* **68**, 733 (1996).
6. A. Hache *et al., Phys. Rev. Lett.* **78**, 306 (1997).
7. P. C. M. Planken *et al. Phys. Rev. B* **48**, 4903 (1993).
8. R. N. Zare, *Science* **279**, 1875 (1998); W. S. Warren, H. Rabitz, M. Dahleh, *ibid.* **259**, 1581 (1993).
9. F. Wang, C. Chen, D. S. Elliot, *Phys. Rev. Lett.* **77**, 2416 (1996).
10. D. M. Meekhof *et al., ibid.* **76**, 1796 (1996).
11. J. A. Yeazell and C. R. Stroud Jr., *ibid.* **60**, 1494 (1988).
12. T. C. Weinacht, J. Ahn, P. H. Bucksbaum, *ibid.* **80**, 5508 (1998); *Nature*, in press.
13. M. U. Wehner, M. H. Ulm, D. S. Chemla, M. Wegener, *ibid.*, p. 1992.
14. P. G. Huggard *et al., Appl. Phys. Lett.* **71**, 2647 (1997).
15. A. P. Heberle, J. J. Baumberg, K. Kohler, *Phys. Rev. Lett.* **75**, 2598 (1995); X. Marie *et al., ibid.* **79**, 3222 (1997).
16. D. Gammon *et al., ibid.* **76**, 3005 (1996).
17. D. Gammon, E. S. Snow, D. S. Katzer, *Appl. Phys. Lett.* **67**, 2391 (1995).
18. N. H. Bonadeo *et al., Phys. Rev. Lett.* **81**, 2759 (1998).
19. S. V. Goupalov, E. L. Ivchenko, A. V. Kavokin, *J. Exp. Theor. Phys.* **86**, 388 (1998).
20. N. F. Scherer *et al., J. Chem. Phys.* **95**, 1487 (1991).
21. H. Metiu and V. Engel, *J. Opt. Soc. Am. B* **7**, 1709 (1990); J. T. Fourkas *et al.*, **6**, 1905 (1989).
22. F. Spano, M. Haner, W. S. Warren, *Chem. Phys. Lett.* **135**, 97 (1987).
23. V. Blanchet, C. Nicole, M.-A. Bouchene, B. Girard, *Phys. Rev. Lett.* **78**, 2716 (1997).
24. U. Bockelmann, *Phys. Rev. B* **48**, 17637 (1993).
25. M. M. Salour and C. Cohen-Tannoudji, *Phys. Rev. Lett.* **38**, 757 (1977); L. D. Noordam, D. I. Duncan, T. F. Gallagher, *Phys. Rev. A* **45**, 4734 (1992).
26. Because the X'- and Y'-oscillator strengths are different, complete cancellation is not observed at the nodes.
27. J. M. Kikkawa, I. P. Smorchkova, N. Samarth, D. D. Awschalom, *Science* **277**, 1284 (1997); J. M. Kikkawa and D. D. Awschalom, *Phys. Rev. Lett.* **80**, 4313 (1998).
28. U. Bockelmann and G. Bastard, *Phys. Rev. B* **42**, 8947 (1990).
29. D. S. Citrin, *Phys. Rev. B* **47**, 3832 (1993).
30. T. Mossberg, A. Flusberg, R. Kachru, S. R. Hartman, *Phys. Rev. Lett.* **42**, 1665 (1979); B. Young, M. Kasevich, S. Chu, in *Atom Interferometry*, P. R. Berman, Ed. (Academic Press, New York, 1997).

31. We thank P. H. Bucksbaum and R. Merlin for stimulating discussions. Supported by U.S. Army Research Office, Air Force Office of Scientific Research, Office of Naval Research and NSF (Center for Ultrafast Optical Science). J.E. was supported by the Danish Research Council.

10 July 1998; accepted 16 September 1998

Photonic Band Gap Guidance in Optical Fibers

J. C. Knight, J. Broeng,* T. A. Birks, P. St. J. Russell

A fundamentally different type of optical waveguide structure is demonstrated, in which light is confined to the vicinity of a low-index region by a two-dimensional photonic band gap crystal. The waveguide consists of an extra air hole in an otherwise regular honeycomb pattern of holes running down the length of a fine silica glass fiber. Optical fibers based on this waveguide mechanism support guided modes with extraordinary properties.

Photonic band gap (PBG) structures offer the opportunity to design new optical properties into existing materials by wavelength-scale periodic microstructuring of the material morphology (*1*). In three-dimensionally periodic PBG materials, waves of certain frequencies cannot enter into or propagate through the material (*1*). In two-dimensionally periodic materials, there can be ranges of the propagation constant normal to the periodic plane (β) where propagation is forbidden (*2, 3*). One potential application of such materials is a type of optical waveguide where light is confined by surrounding it with a band gap material (*4*). Two-dimensionally periodic structures in the form of long, fine silica fibers that have a regular array of tiny air holes running down their length (*3, 5–8*) constitute artificial two-dimensional "crystals" with lattice constants on the order of micrometers. We previously demonstrated an optical fiber waveguide based on total internal reflection from this periodic material—a waveguiding mechanism very similar to that in conventional optical fibers (albeit with some remarkable features) (*5–8*). We now report the realization and demonstration of a far more radical optical fiber design, based on light confinement by the PBG effect.

Our fabrication process is related to that reported by Tonucci *et al.* (*9*) and involves stacking a few hundred solid silica rods and silica capillary tubes by hand in a hexagonal arrangement to form a fiber preform, which is then drawn down at a temperature of around 2000°C to a fiber with a diameter of about 40

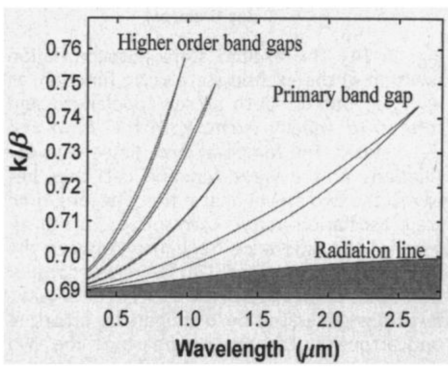

Fig. 1. Computed band gaps in the air-silica honeycomb lattice being discussed here. The parameters used in the computation were a nearest hole spacing of 1.9 μm and an air hole diameter of 0.55 μm.

Optoelectronics Group, Department of Physics, University of Bath, Claverton Down, Bath BA2 7AY, UK.

*Visiting from the Department of Electromagnetic Systems, Technical University of Denmark, 2800 Lyngby, Denmark.

μm. The submicrometer-sized air holes in the final fiber are spaced by a few micrometers. Previous fibers were based on a simple hexagonal array of air holes, made by stacking tubes only. However, we did not observe band gap guidance in a hexagonal structure. Our attention switched to a honeycomb array of holes, which is known to show broader band gaps for in-plane (*10*) as well as for out-of-plane (*11*) propagation. Calculations with the plane-wave method show that for realizable scales of structures and air-filling fractions, we expect to observe band gaps at visible light frequencies in ideal structures (*11*). This is true for out-of-plane propagation, even though the air-filling fraction and refractive index contrast are too small to observe band gaps in the periodic plane (*3*). Calculations for the parameter range investigated experimentally (Fig. 1) show that band gaps appear for a wide range of wavelengths for values of k/β above the "radiation line," below which one expects to find total reflection from the structure (k is the vacuum wavenumber). To create a waveguiding "core," one needs to introduce a "defect" into the crystal structure—a localized region with optical properties different from those of the fully periodic structure. This core is surrounded by a "cladding"—the fully periodic region—the purpose of which is to confine the light within the core. Within a properly designed defect, light can propagate with a value of β that falls within the band gap of the surrounding cladding material. Further numerical modeling shows that by introducing an "extra" air hole into a single lattice site within the structure, localized guided modes can appear within the band gaps (*11*), in certain wavelength ranges.

Experimentally, the honeycomb structure is created by individual positioning of rods as well as capillaries in the stacking stage. An extra air hole is introduced into the center of the honeycomb pattern by replacing a single solid rod with a hollow capillary. This "low-index defect" ensures that there is no possibility of waveguiding by total internal reflection (*6*). Because the capillaries and rods are circular in cross section but are stacked into a hexagonal array, there are small air gaps—interstitial holes—that are formed within the structure. These interstitial holes collapse during the fabrication process under surface tension forces, surviving near to the center of the fiber after they have disappeared elsewhere because of the extra forces that result from the presence of the extra air hole (Fig. 2). They appear to play an important role in the optical properties of the samples.

We observe a guided mode in the core of the structure (Figs. 3 and 4). The observed effects are highly sensitive to the precise structure and scale of the core and cladding and are not observed for a range of fibers with slightly different parameters. Small variations in the structure of the fiber over lengths on the order of 10 cm (which are due to variations in conditions within the furnace during fiber drawing) cause the waveguiding properties to change substantially or even to disappear completely. Nonetheless, we can reproducibly fabricate samples that look like that in Fig. 2 and that demonstrate the same optical effects. We are as yet unable to quantitatively model the fabricated structures (Fig. 2). The air holes in our samples are not round (as in our calculations) but are distorted by the effects of surface tension. More problematic are the interstitial air holes within the "core" of the fiber, which have not been modeled accurately because they are so small. However, the band gap plot for the corresponding ideal structure (Fig. 1) does show several band gaps at the visible wavelengths at which we observe waveguiding. The exact frequencies at which theory predicts confined waveguide modes depend on the design of the defect as well as that of the periodic structure, and their determination requires precise modeling of the structure under study.

To demonstrate that these features (Fig. 3) are due to a single guided mode, we focused visible laser light onto one end of lengths (about 50 mm) of the fiber using a high-power objective lens. Near-field and far-field patterns at the output end were observed (Fig. 4). The relative intensities of the six lobes in the near-field pattern (Fig. 4A) remained fixed as the input coupling was varied and are nearly equal. No other mode field patterns are observed confined to the defect region. The guided mode is tightly confined to a small silica region that is directly connected to a much larger one (Figs. 2 and 4A), demonstrating the unusual nature of the waveguiding process.

The six-lobed far-field pattern (Fig. 4B) remains fixed and unchanging with input coupling, except that the overall intensity of the pattern is extremely sensitive to the precise input coupling. The far-field pattern diverges at an angle of about 25° with respect to the fiber axis, and a similar angle was used for the input coupling. It is worth remarking that the observed far-field intensity pattern (Fig. 4B) can only arise from the near-field intensity pattern (Fig. 4A) by postulating that the fields in opposite lobes of the field pattern have opposite signs. The computed guided-mode profile presented in (*11*) showed no such phase reversals. However, we found that modal field patterns with a similar symmetry to that observed experimentally can be computed in higher order band gaps. This is consistent with the observation that the mode presented in (*11*) was computed for a wavelength of 1.5 μm, whereas the mode observed here is guided at about one-third of that wavelength in a structure with a similar scale. The fiber shown (Figs. 2 and 3) guided light for wavelengths between at least 458 and 528 nm (argon-ion laser lines). No confined mode could be observed at a wavelength of 633 nm (helium-neon laser), despite exhaustive attempts. Modal field patterns similar to that in Fig. 4A could be observed by

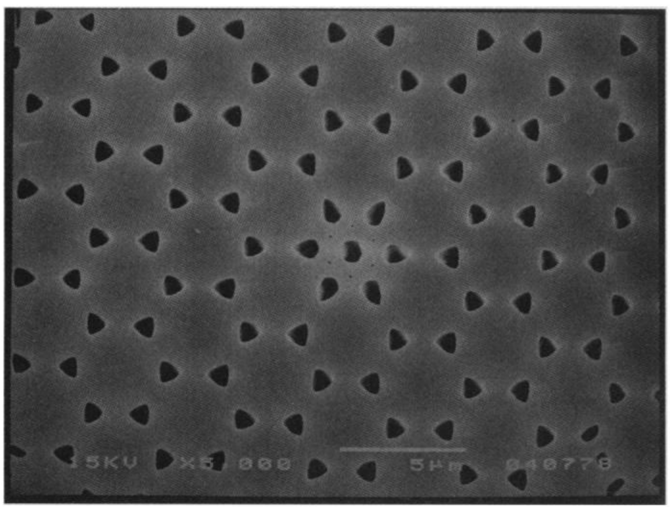

Fig. 2. Scanning electron micrograph of the surface of a cleaved PBG fiber waveguide 5 cm long. The parameters of the fiber shown are a diameter of 36 μm, a nearest air hole spacing of 1.9 μm, and an air-filling fraction in the periodic region of 5.3%. The central air hole is 0.8 μm in diameter and is surrounded by six interstitial holes of diameter of about 75 nm. This fiber guides light at between at least 458 and 528 nm, but not at 633 nm.

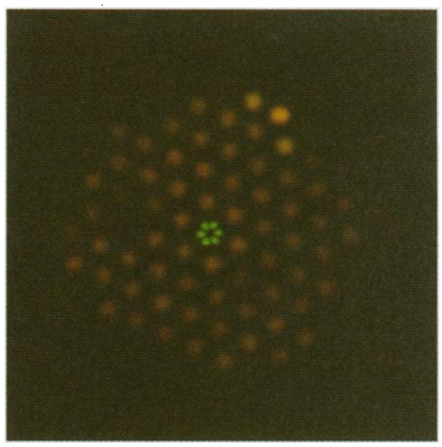

Fig. 3. Optical micrograph of a PBG fiber. The fiber is illuminated from below with a white light source, and index-matching fluid on the sides of the fiber is used to strip off some of the light in cladding modes. The fiber shown guides blue and green light in the low-index core.

focusing the light onto the core region, but they were always accompanied by substantial light that filled the whole fiber. No indication of a far-field pattern like that in Fig. 4B was observed. A relatively sharp transition—with wavelength—from a confined to a nonconfined mode is expected to be a feature of this type of waveguiding.

Some qualitative insight into the nature of the guided modes being described here can be gained by considering the honeycomb structure shown in Fig. 2 as a large number of independent silica strands that are strongly coupled together. Each isolated strand would support many distinct waveguide modes, each with a different value of β. When a large number of strands are placed in close proximity, they couple together, and each mode of the single strand opens up into a passband of modes of the composite structure, each passband now covering a range of β values. The passbands are separated by band gaps. The central silica strand (the "core"), which has a large hole in the middle and six smaller interstitial holes disposed symmetrically around it, would, if isolated, support a different set of waveguide modes because of its different morphology. If the β value of one of these modes falls within one of the bands of modes of the periodic cladding, this mode of the core will be coupled to the extended modes of the periodic cladding. However, if one of the modes of the core region falls in between the passbands of the fully periodic cladding region, then this mode is localized within the core and forms a PBG guided mode. Thus, at some wavelengths, there is a mode trapped within the core (the "guided mode"), whereas at other wavelengths the modes are extended and fill the fiber. A possible reason for the importance of the hard-to-model interstitial holes within the core is that they will affect the β values of the core modes, drawing one of these into the band gap of the continuous material.

A

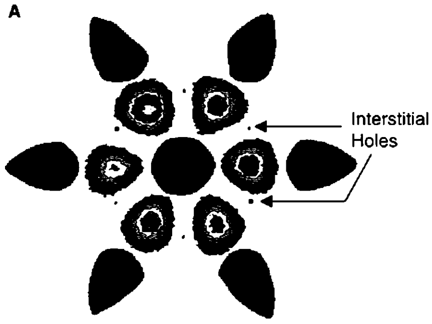

B

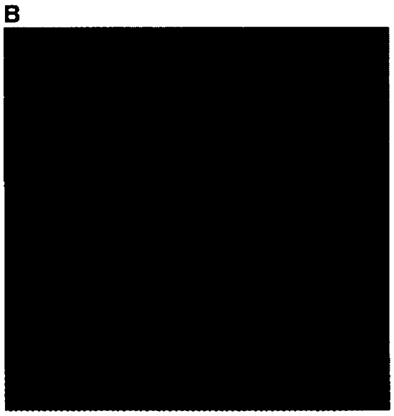

Fig. 4. Near- and far-field patterns observed with laser light (wavelength = 458 nm) to excite the guided mode in a 50-mm length of fiber. **(A)** A contour map of the observed near-field pattern (color) superimposed on a scanning electron micrograph showing the fiber morphology (black). The interstitial holes in the structure (which appear between the lobes of the guided mode) are clearly visible. The guided-mode field intensity outside the first ring of air holes is at least two orders of magnitude less than the peak intensity shown. **(B)** A photograph of the observed far-field pattern. The pattern was recorded by allowing the diffracting light emerging from the end of the fiber to fall onto a paper screen, which was then imaged onto photographic film from the back. The orientation of the six main lobes in the far-field pattern is the same as those in the near field.

Band gap guided modes are expected to have quite different properties to the modes of conventional optical waveguides. For example, we observe that the fiber being described here is strongly birefringent, with a beat length on the order of millimeters (that is, the different polarization modes have rather different propagation constants). We conclude that small imperfections in the structure can have a large effect on the propagation constant of the trapped modes. The dispersion of these fibers is likely to be far larger than that observed in any previous optical fiber waveguide for the correct choice of fiber design parameters. Other properties of these fibers (for example, their susceptibility to bend loss) remain to be investigated, and even more counterintuitive designs (a silica-air waveguide where the light is trapped within an air hole, for example) are possible. This is only the first of a very broad class of fiber guided modes, which show great technological promise and are of substantial scientific interest.

References and Notes

1. E. Yablonovitch, *J. Opt. Soc. Am. B* **10**, 283 (1993).
2. P. St. J. Russell, D. M. Atkin, T. A. Birks, P. J. Roberts, in *Microcavities and Photonic Bandgaps: Physics and Applications*, J. G. Rarity and C. Weisbuch, Eds. (Kluwer, Dordrecht, Netherlands, 1996), pp. 203–218.
3. T. A. Birks, P. J. Roberts, P. St. J. Russell, D. M. Atkin, T. J. Shepherd, *Electron. Lett.* **31**, 1941 (1995).
4. J. D. Joannopoulos, R. D. Meade, J. N. Winn, *Photonic Crystals: Molding the Flow of Light* (Princeton Univ. Press, Princeton, NJ, 1995).
5. J. C. Knight, T. A. Birks, P. St. J. Russell, D. M. Atkin, *Opt. Lett.* **21**, 1547 (1996) [errata: *ibid.* **22**, 484 (1997)].
6. T. A. Birks, J. C. Knight, P. St. J. Russell, *ibid.*, p. 961.
7. J. C. Knight, T. A. Birks, P. St. J. Russell, J.-P. de Sandro, *J. Opt. Soc. Am. A* **15**, 748 (1998).
8. J. C. Knight, T. A. Birks, R. F. Cregan, P. St. J. Russell, J.-P. de Sandro, *Electron. Lett.* **34**, 1347 (1998).
9. R. J. Tonucci, B. L. Justus, A. J. Campillo, C. E. Ford, *Science* **258**, 783 (1992).
10. D. Cassagne, C. Jouanin, D. Bertho, *Phys. Rev. B* **53**, 7134 (1996).
11. J. Broeng *et al.*, *Opt. Commun.* **156**, 240 (1995).

12. Supported by the Defence Evaluation and Research Agency, Malvern, UK, and the UK Engineering and Physical Sciences Research Council. Donation of fiber-drawing equipment from BT Research Laboratories, Martlesham, UK, is gratefully acknowledged.

25 August 1998; accepted 14 October 1998

Direct Demonstration of Milk as an Element of Archaeological Economies

Stephanie N. Dudd and Richard P. Evershed*

The stable carbon isotope ($\delta^{13}C$) compositions of individual fatty acid components of remnant fats preserved in archaeological pottery vessels show that dairying was a component of archaeological economies. Characteristic $\delta^{13}C$ values arise from biases in the biosynthetic origins of the $C_{18:0}$ fatty acids in milk and adipose fat. Milk and adipose fat from animals raised on similar pastures and fodders have distinct isotopic signatures.

Although sheep are thought to have been domesticated in the Near East at ~9000 B.C. and cattle and goats were domesticated at ~7000 B.C., there is no direct evidence that they were milked. Pictorial and written records from the Sahara, Egypt, and Mesopotamia show that dairying had begun there by 4000 to 2900 B.C. (*1*). Evidence of dairying during the prehistoric period in Britain has been limited solely to secondary evidence associated with the procurement and use of dairy products, such as putative ceramic "cheese" strainers, dating from 4500 B.C. (*2*, *3*). Faunal studies have suggested that a high neonatal cull and a bias in the adult cull in domestic ruminant animals may indicate dair-

Organic Geochemistry Unit, School of Chemistry, University of Bristol, Cantock's Close, Bristol, BS8 1TS, UK.

*To whom correspondence should be addressed. E-mail: r.p.evershed@bristol.ac.uk